Soft Matter

RSC Publishing

PAPER

View Article Online
View Journal | View Issue

Yielding and flow of concentrated Pickering emulsions†

Cite this: *Soft Matter*, 2013, **9**, 7568

Michiel Hermes* and Paul S. Clegg*

We have used rheo-imaging to investigate the shear flow of particle-stabilized (Pickering) emulsions with different interactions between droplets. To minimize creaming, we have worked with arrested networks of droplets. We observe three different yielding mechanisms as well as shear thickening at high strain. Pickering emulsions comprised of repulsive droplets respond to small strains initially by reversible movement, then, as the strain is increased, yielding occurs *via* cage breaking. At large strains there is a peak in both moduli and correlations between droplet trajectories indicative of shear thickening and jamming. Pickering emulsions comprised of attractive droplets share similar features and additionally have a loss modulus peak at low strain associated with the breakage and rearrangement of the attractive bonds. We observe that small attractive droplets already start to move irreversibly at small strains even though yielding has not yet occurred. As the strain is increased, the percolating network of larger droplets is eventually completely broken and the sample yields as a whole. Finally, we explore what happens when a highly compressed emulsion or bi-liquid foam is subjected to shear flow: we find that at high strain the particles fail to stabilize the interface and the emulsion is destroyed.

Received 29th March 2013
Accepted 17th June 2013

DOI: 10.1039/c3sm50889g

www.rsc.org/softmatter

Introduction

Emulsions are dispersions of droplets in a host solvent and their flow properties can strongly differ from those of dispersions of solid particles.[1] Typically, the droplet interfaces are stabilized by the presence of some surface active species (*e.g.* surfactants, protein molecules or small particles) and these can modify the flow properties by modifying the interactions between the droplets and/or the interfacial rheology of the droplets themselves. Many common foods and cosmetics, for example, are emulsions and they are also encountered in crude oil and waste water treatment. Hence, an understanding of emulsion flow properties is of both fundamental interest and of value for many applications.

Pickering emulsions are comprised of droplets stabilized by colloidal particles instead of, the more common, surfactant molecules.[2–5] The interfacial attachment energy for a surfactant molecule is several k_BT therefore the interfacial population is always in a dynamic equilibrium with a population in the host solvent. Colloidal particles, on the other hand, need to overcome an energy barrier of hundreds or thousands of k_BT to detach from the interface. This huge energy barrier makes Pickering emulsions, once fully covered in particles, extremely stable.[4] A further advantage of particle-stabilization is that the interactions between colloidal particles are very well understood and can be tuned *via* chemical modification, index matching and the addition of salt or non-adsorbing polymers. This understanding can be deployed to modify the interactions between emulsion droplets.

The rheology and yielding behavior of surfactant-stabilized emulsions has been studied extensively.[6–10] If at all, these studies used indirect methods to obtain information about the microscopic droplet dynamics. Here we combine rheology with real space imaging using a confocal microscope so that we can correlate the strain induced microscopic rearrangements with the bulk shear flow properties of Pickering droplets. Several studies have probed the flow properties of Pickering emulsions without imaging.[11–15] These studies focused on systems dominated by attractive interactions between droplets, hence the emulsions exhibited a yield stress at relatively low volume fraction. A key feature, compared to typical surfactant-stabilized emulsions, was that shear thickening was found at high volume fraction.[13] It was suggested that this was a symptom of an underlying similarity between Pickering emulsion rheology and hard sphere rheology. Additionally, extensional and compressional rheology studies have revealed the droplet break-up[16] and the droplet–droplet contact behavior[11,17] of Pickering emulsions, respectively.

Many soft materials yield from being solid-like to fluid-like in response to an increase in applied stress; this transition gives rise to a large deformation and is associated with irreversible changes to the internal structure of the solid. Yielding can be viewed as an 'unjamming' process in line with the general jamming diagram.[18,19] For example, hard colloidal particles at high volume fraction will respond as a solid to a small strain but will be pushed out of their cages and start flowing at moderate strain. This is a yielding process and the details of how it occurs

School of Physics and Astronomy, University of Edinburgh, Mayfield Road, Edinburgh, EH9 3JZ, UK. E-mail: m.hermes@ed.ac.uk; paul.clegg@ed.ac.uk

† Electronic supplementary information (ESI) available. See DOI: 10.1039/c3sm50889g

change as the interactions between the particles are modified.[20] When the strain on a fluidized system of hard particles is increased even more they will start to jam and shear thicken.[21–23] This is caused by collisions with neighboring particles and the formation of system spanning clusters of particles.

Large differences have been reported between the flow and yielding behavior of attractive gel-like systems and repulsive glassy systems.[9,10,20,24] None of these studies have investigated the microscopic origins of these differences; in spite of which, they have associated bulk characteristics, such as the variation in the loss modulus G'' as the strain is increased, with microscopic phenomena such as bond breaking, cage breaking, jamming and yielding.[10,20,25] Here we show in real space what happens before, during and after the yielding of particle-stabilized emulsions. By coating the droplet interfaces with silica particles, for which we can control the interactions, we are able to probe a repulsive glass-like state, an attractive emulsion gel and a dense bi-liquid foam in turn.

Materials and methods

The silica particles were 660 nm in diameter with a polydispersity of 16% and had been fluorescently labeled with rhodamine. The particles were dried in a vacuum oven at 120 °C for 60 minutes and then re-dispersed in distilled water by sonication in a bath for 30 minutes. Silica stabilized emulsion where made by adding a mixture of 42.5%$_w$ dodecane and 57.5%$_w$ sunflower oil followed by mixing using a vortex mixer for 60 seconds (the oil mixture was saturated with Nile red and filtered before the mixing step). This resulted in emulsions with an average droplet size between 15 and 30 μm and a polydispersity of approximately 30%. We had to dry the silica particles or add salt to the dispersion to facilitate interfacial trapping.[26] After the emulsions were made Glycerol or NaI was added to index match the system. These emulsions were subsequently centrifuged at 2000 rpm for 30 minutes. The continuous phase was pipetted from the bottom, weighed and stored. These emulsions were stable for several months at least. When the emulsions were used they were diluted with the continuous phase to obtain the required volume fraction of oil, as determined from the weight ratio of oil to water mixture. The emulsions were homogenized by gentle shaking prior to loading in the rheometer.

At high salt concentrations the silica particles form an attractive gel[27] that can be seen to deform, break up and reform under steady shear flow. With these attractive silica particles at the droplet surface the droplets form an attractive gel.[28] The individual silica particles on the interface of the oil droplets can also be imaged close to the cover slide; during flow they rearrange and move on the interface. The droplets themselves can be seen to bend and deform considerably without any cracks or sudden rearrangements of particles at the interface.

The imaging was performed on a VT-Eye confocal microscope using a 560 nm laser for the rhodamine and a 480 nm laser for the Nile red. An Anton Paar MCR301 rheometer was mounted over the confocal microscope frame.[29] The cone employed has a diameter of 5 cm, a 1° angle, a truncation gap of 100 μm and was sandblasted to a roughness average Ra = 4.37 μm with a maximum profile Rz = 33.8 μm. The glass bottom plate was made rough by a coating of fine sand containing (clusters of) grains between 10 and 100 μm in diameter attached with UV curing glue. A tiny bit of the sand was removed to facilitate good imaging. The sample was gently poured and spread on the glass plate and the cone was lowered slowly to avoid destruction of the structure, Fig. 1. The gap height was set using the normal force and checked using the confocal microscope. When the system deviates from linearity, at large strains, the response function is no longer sinusoidal. Hence, G' and G'' as given by the rheometer software no longer describe the complete response function of the system. When this is the case G' and G'' obtained in this way remain mathematically well defined but the physical interpretation becomes less straight forward.[30,31] We augment these numbers with a physical interpretation from our images.

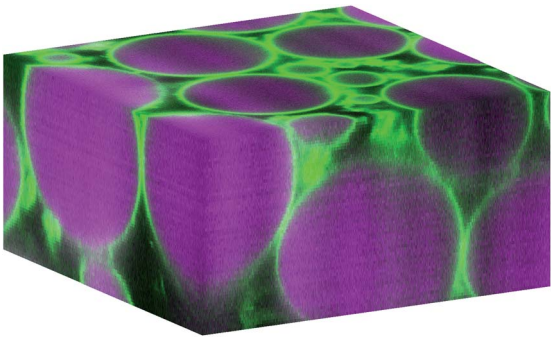

Fig. 1 Confocal images of oil droplets stabilized by silica particles shown with false colours. The (volume) average size of the oil droplets is 25 μm, the polydispersity is approximately 30% and the average diameter of the silica is 660 nm. The silica is colored green (rhodamine), the oil is colored pink (Nile red) and the water is unlabeled and black. The imaged volume is 64 × 64 × 30 μm.

To quantify changes to the images during flow the maximum Pearson correlation,[32] r, between image X and image Y was calculated:

$$r = \frac{1}{n-1}\sum_{i=1}^{n}\left(\frac{X_i - \overline{X}}{s_X}\right)\left(\frac{Y_i - \overline{Y}}{s_Y}\right). \quad (1)$$

The sum is over all paired pixels X_i and Y_i, s_X is the standard deviation and $\bar{X}$ is the mean of X. The maximum is found by shifting the images relative to each other and pairing the overlapping pixels. To obtain sub-pixel accuracy the peak is fitted with a second order polynomial to find the maximum. To speed up the calculation, image shifting and maximum fitting were only performed in the velocity direction. This technique of measuring the correlation between images to quantify the motion between images can be seen as the real space analog of the diffusive wave spectroscopy (DWS) technique used in refs. 8, 33, 34.

The droplets in this study are too large to show any significant Brownian motion, *i.e.* the gravitational Peclet number $\frac{4\pi g \Delta\rho R^4}{3k_B T} \gg 1000$; hence, they are granular in nature and all movements are caused by the externally supplied driving force. Because of the strong effect of gravity we had to take steps to

avoid vertical stratification (creaming) dominating our experiments, *i.e.* we can only characterize the flow properties in jammed or otherwise arrested states. Even in these states care is required due to the significant gradient in the cumulative buoyancy force up the sample.

Results

In Fig. 2a the elastic or storage modulus G' and viscous or loss modulus G'' of a repulsive emulsion at $65 \pm 2\%_v$ are shown. The volume averaged droplet size[1] d_{43} is 25 μm and the oscillation frequency is 1 Hz. At strain amplitudes $\gamma < 0.1\%$ the systems responds purely elastically and both G' and G'' do not depend on the strain amplitude. If flow involved the distortion of a large proportion of droplets then $G' > \Gamma/d_{43} \sim 1000$ Pa (where Γ is the interfacial tension) which we are significantly below. This linear regime lasts until a strain of ≈0.1% when G' starts to decrease. At strain amplitudes $0.1\% < \gamma < 10\%$ the droplets slide along each other but remain trapped in the cages formed by their neighbors. The emulsion retains a solid-like character with $G' > G''$. Although the drops can be seen sliding and rolling against each other (Fig. 2b and ESI movie 4 and 5†), all movement is reversible as evidenced by the lack of visible difference between pictures taken at the same phase of the oscillation. At a strain of approximately 10% the moduli cross and the droplets can be seen to move irreversibly as shown in Fig. 2c and ESI movies 4 and 5.† Motion is limited: the droplets move much less than their diameter in one period (one second). After this crossing point both G' and G'' keep decreasing till a strain of 30% after which both start to increase due to jamming which results in shear thickening. There is a single point when G'' is maximal at a strain of approximately 110%. At this point the droplets move rapidly, their own diameter or more per period (one second) the small droplets seem to have more freedom than the big drops and move more. At strains higher than 130% both G' and G'' seem to follow a power law with G' a power that is approximately 2.2 ± 0.2 that of G'' slightly deviating from the factor of two[10,35,36] as has been observed before.[37] When at the end of the experiment the shear is stopped the system relaxes quickly, within several seconds, to a jammed immobile state. Some free silica particles can be seen to move around occasionally forming small clusters indicating that the particles did not perfectly redisperse after drying.

To analyse these image sequences we also calculated the Pearson correlation between frames. (Because the background of these images is slightly grey the Pearson correlation does not decay all the way to zero but to approximately 0.2–0.4 for the case of uncorrelated droplet coordinates.) In Fig. 2e the correlation between frames at one extrema of the oscillation are presented for different strain amplitudes. By comparing frames at the same phase of the oscillation we measure the amount of irreversible motion. For strain amplitudes less than 6% the decay in the correlation over time is very small and mainly caused by the movement of the free silica particles. For larger amplitudes the decay is suddenly much larger. The correlation between two frames one period (of one second) apart is shown inset to Fig. 2e for different strain amplitudes (see legend). The

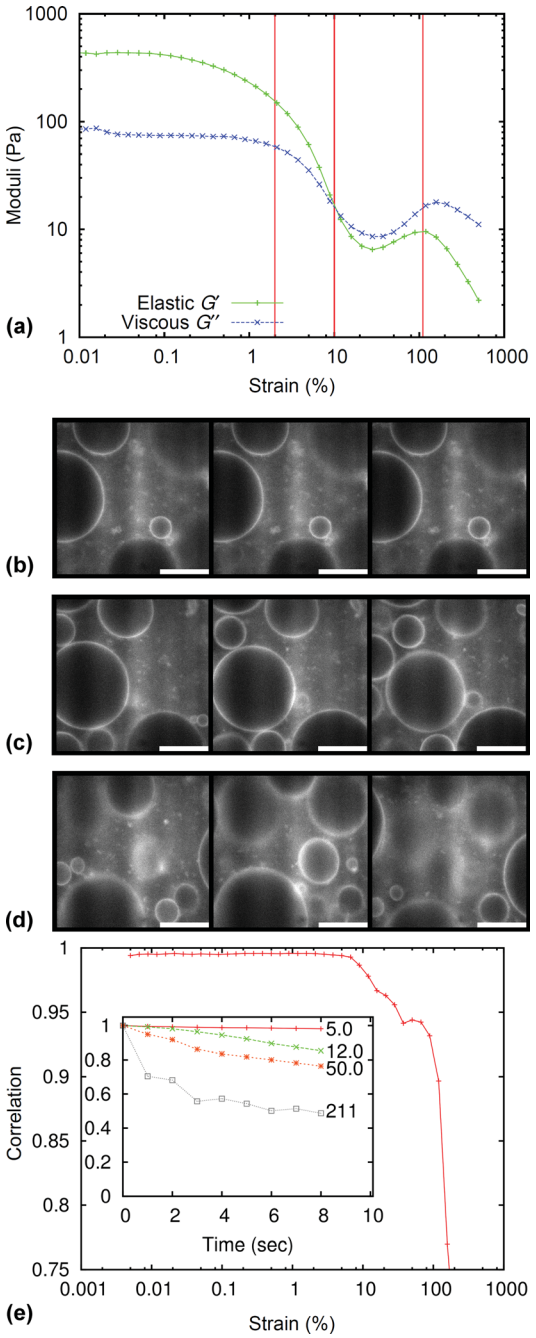

Fig. 2 (a) The shear moduli of a Pickering emulsion stabilized by silica colloids. The volume fraction of the oil is 65%. No salt is added so the interactions between the droplets are repulsive. (b–d) Confocal images of the emulsion during the shear taken 40 μm into the sample to avoid wall effects. All scale bars are 20 μm. (b) Strain 1.5%; (c) strain 15%; (d) strain 110%. (e) The average correlation between two frames one period apart as function of the strain amplitude. Inset: the decay of the correlation between frames at the same phase of the oscillation for different amplitudes.

first point where G'' is larger than G' is very close to the point when the decay of the correlation falls precipitously. So this shows, as we already saw from the pictures, that cage breaking starts to occur when the moduli cross. We verified that the results do not depend on the position in the sample by repeating the analysis at another z position. This demonstrates

that, for repulsive droplets, the yield strain, defined as the crossing point of G' and G'' coincides with the strain where the first irreversible motion occurs. After the peak in the moduli at $\approx$100% strain the correlation plummets very steeply again. This is caused by the break up of the jammed structure that was causing the shear thickening behavior.

In other experiments, carried out for volume fractions below 0.58, the sample creams and we observe a very strong shear localization due to the resulting density gradient (data not shown). During all measurements which make up Fig. 2a we have examined the flow profile. While there are strong local fluctuations, on average the flow profile was always linear *i.e.* there was no shear banding or slip; here we agree with the results of Bécu *et al.*[9] for non-adhesive emulsions. However, when the system has been left to age and sediment for a couple of hours even at volume fractions above random close packing a density gradient is set up (this is consistent with the slow intermittent rearrangements observed previously in dense Pickering emulsions[38]). When we do not perform any pre-shear on these aged samples the sample does not yield homogeneously but yields first at the bottom, where the density of the droplets is lowest, while the top remains immobile.

In Fig. 3a the typical storage and loss moduli of an attractive Pickering emulsion gel are shown. The average droplet size is 15 μm, the salt concentration in the continuous phase is 44.8%$_w$ and the volume fraction of oil is 50%$_v$; again the oscillation frequency is 1 Hz. Both moduli follow a linear plateau until $\approx$0.1% strain after which G' starts to decrease and G'' shows a slight increase. At a strain of 1% all movement is reversible and we did not observe any droplets becoming detached from each other, however, we did see silica particles making and reforming contacts on neighboring droplets. In Fig. 3b three pictures taken one period apart are shown and it can be seen that at a strain of 10% the small droplets move irreversibly and exchange which neighbors they are bonded to while the large droplets return to the same position. The small droplets break their bonds at lower strain because of the correspondingly smaller contact area. The larger droplets also have a lower Laplace pressure and thus may be more flexible.

At a strain of 50%, G' and G'' cross and even the large droplets start to move irreversibly (they have escaped their cages). ESI movie 1 and 2† and in Fig. 3c show this fast movement. (The droplet in the top right corner is stuck to the bottom wall.) There are no free silica particles because of the attraction, however, there are small clusters of silica particles stuck to the droplets. It is not easy to further quantify the contact area and thus the bond breaking between droplets from the images since it is difficult to distinguish between movement out of the imaging plane and bond breaking. We show images close to the stationary bottom wall because higher in the sample the global movement results in a much larger motion of the droplets making it difficult to observe the (absence of collective) relative motion. We did not observe the shear banding or solid liquid coexistence observed by Bécu *et al.*[9] in the case of attractive emulsions. We also did not observe the second decrease in the correlation at the shear thickening peak, Fig. 3d. This is most likely because this peak is so much lower and the shear

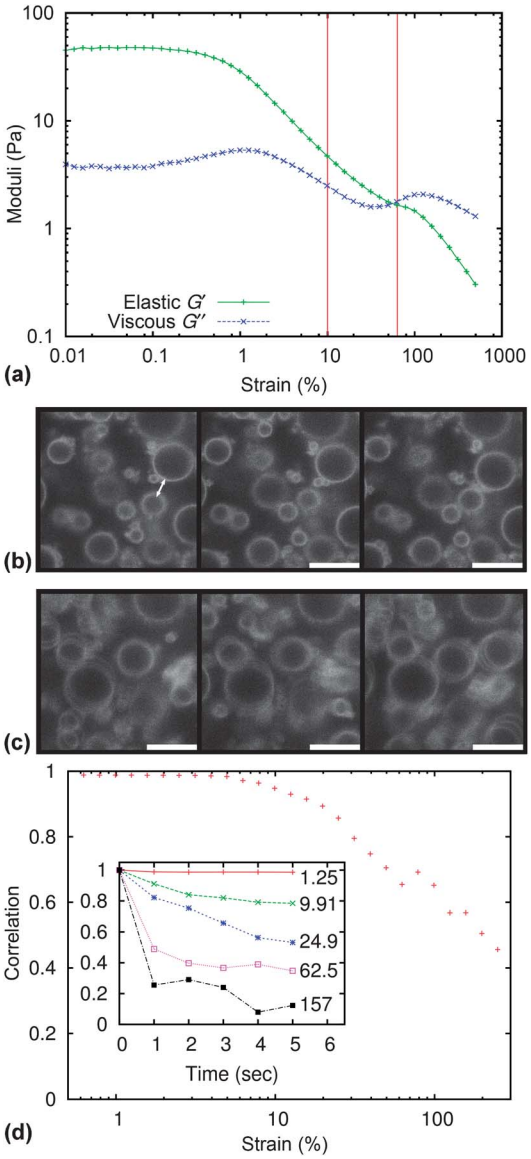

Fig. 3 (a) The moduli as a function of strain amplitude for a gel-like Pickering emulsion comprised of 50%$_v$ of attractive droplets. (b and c) Images taken one period (one second) apart at a height of 20 μm. To convey movement or lack thereof we averaged over three frames taken 0.03 seconds apart. All scale bars are 20 μm. (b) Strain 10%; (c) strain 63%. (d) The average correlation between two frames one period apart as function of the strain amplitude. Inset: the decay of the correlation between frames at the same phase of the oscillation for different amplitudes.

thickening is too subtle to have a clear signature in the decay of the correlation. Alternatively, the most pronounced clustering may well be in the gradient direction, *i.e.* out of our image plane.[39] At strains higher than 130% both G' and G'' seem to follow a power law with G' a power that is approximately 2.5 $\pm$ 0.2 that of G''.

Inset to Fig. 3d the decay of the correlation between frames one period apart is shown as a function of time. The shape of these curves differs significantly from those of the repulsive glass emulsion inset to Fig. 2e (note the different scale). The movement of the droplets is much faster once their bonds are broken and we do not observe the collective movement which

we observed in the glassy samples. As already seen from the images, the onset of irreversible motion does not correspond with the macroscopic yield point since the smaller droplets already move irreversibly at strains of ≈5% while the macroscopic yield point defined by the crossing of G' and G'' lies at a strain of ≈55%.

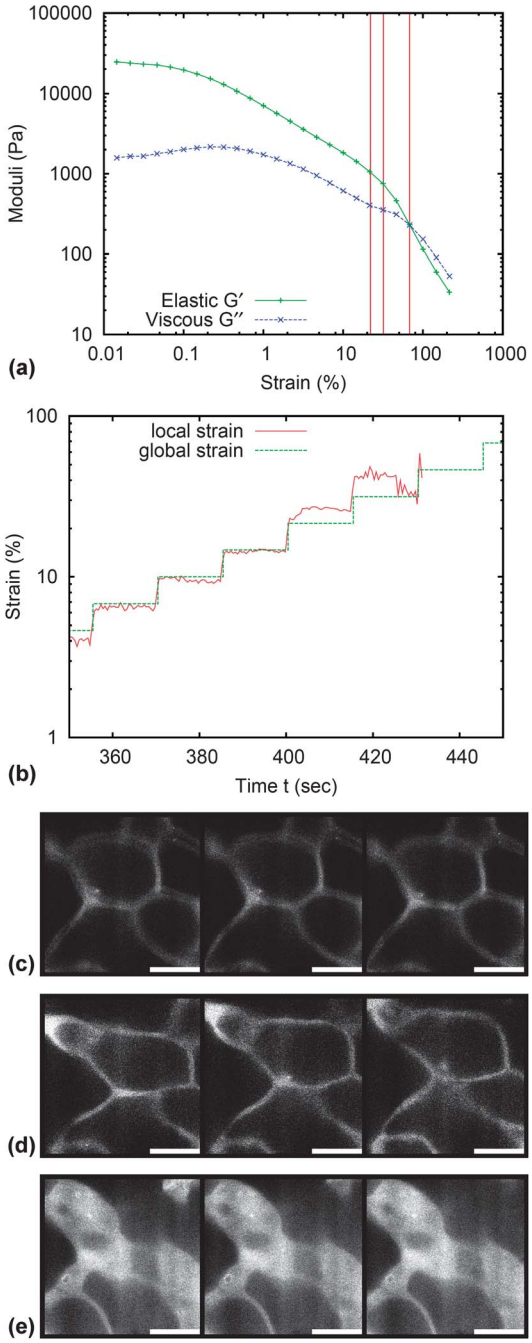

Fig. 4 (a) The moduli as a function of strain amplitude for a bi-liquid foam comprised of ≈95%$_v$ of Pickering emulsion droplets. (b) The local strain at a height of 20 μm obtained from the images. After 430 seconds at a strain of 46% the bottom part of the image stops moving completely and disconnects from the mobile top right. (c–e) Images at a height of 20 μm. All scale bars are 20 μm. (c) One second apart, strain 22%. To demonstrate the movement we have overlapped 2 frames 0.1 seconds apart. (d) One second apart, strain of 32%. (e) 0.5 seconds apart, strain of 68%.

To investigate the effect of irreversible structural change we compressed an attractive emulsion with an average droplet diameter of 20 μm to a bi-liquid foam by centrifugation. This foam, oil volume fraction ≈95%, was very carefully spread on the plate of the rheometer. In Fig. 4a we plot the moduli for an increasing strain. The first thing to notice is that the emulsion has become very stiff and that G' is two orders of magnitude larger than the emulsion in Fig. 2. This scale of modulus corresponds to $\Gamma/d \sim 30\,000$ Pa, where d is the particle diameter, which has been suggested as an order of magnitude for the Young's modulus of a particle coated interface.[40] The plateau that was visible in the previous cases has now been pushed to very low strains and already at strains of 0.01% the sample shows non-linear behaviour. A small peak in G'' is visible at a strain of 0.3%. Inspection of the movies indicates that no bonds between droplets are completely broken. This would be very difficult at this high packing fractions and such low strain. However, the contact area between the droplets can be seen to change, mainly in the strongly bent corners: bonds between silica colloids are being broken and re-formed, explaining the increase in dissipation.

In Fig. 4b the local strain amplitude in the total sample is compared with the strain between the bottom plate and the imaging plane. At a strain of 21.5% the local strain suddenly becomes larger than the total strain indicating that the shear is becoming localized, at a strain of 31.6% there are large fluctuations and at a global strain of 46.4% the stability of the droplets in this high shear zone is lost and the droplets coalesce. Silica particles are removed from the interface and end up in one of the two liquid phases.

When the strain was increased to 50%, G' and G'' cross and at this point the emulsion is destroyed. In Fig. 4d and ESI movie 3† the droplets in the top right corner can be seen to merge when the film separating them snaps. A little bit later this happens in more places. In the end only a few original small droplets are left and the rest of the oil is collected in a few very large droplets. All this destruction results, as expected, in a decrease of both G' and G''. Forced coalescence is not uniform throughout the height of the sample but is mainly confined to a small fracture plane in which, after droplet destruction, all the shear is localized.

Discussion

We have reported above storage and loss moduli with accompanying images for repulsive, attractive and very high volume fraction Pickering emulsions. For the different inter-droplet interactions, our observations are consistent with the concepts of cage breaking and bond breaking which are familiar from the rheology of dense colloidal dispersions.[20] For the very high volume fraction Pickering emulsion the added ingredient is the destruction of droplets under shear. Our work extends previous rheology studies of Pickering emulsions to the cases of repulsive droplets and biliquid foams.[11–15] Because we combine rheology with imaging we are able to identify the microscopic processes associated with the bulk signatures. In common with the observations of Wolf *et al.* for micron scale Pickering emulsion

droplets,[13] we have observed a shear thickening signature at large strain amplitudes, here for droplet sizes larger than 10 μm. From our image correlation data Fig. 2e it is possible to associate this with the formation of droplet clusters driven by shear.

It is instructive to compare our Pickering emulsion flow properties to those observed for surfactant-stabilized emulsions.[8–10] Hébraud *et al.* used diffusive wave spectroscopy to distinguish between reversible and irreversible motion of droplets under oscillating shear.[8] They associate the increase in irreversible motion with the onset of yielding. They found that there were two populations of droplets for any given strain amplitude: those that began irreversible motion after the first strain cycle and those whose motion remained reversible for many strain cycles. The proportion of droplets undergoing irreversible motion increased with increasing strain amplitude but decreased with increasing volume fraction of droplets. We have not observed such a strong difference between mobile and immobile droplets at the volume fractions they explore. We do have two populations immediately prior to yielding in our attractive, relatively polydisperse, emulsions; however, this is at a volume fraction where there is more space for small droplets to rattle around.

Bécu *et al.* studied attractive and repulsive emulsions stabilized by surfactants in order to establish whether the local interactions modified the bulk flow properties.[9] They employed ultrasound velocimetry to determine the flow profile of their samples (emulsions of droplet volume fraction 73% in a Couette cell) as a function of shear rate. They observed homogeneous flow for repulsive droplets while strong shear banding across the gap was seen at intermediate shear rates for attractive droplets. Our results suggest that shear banding is not generic for attractive emulsion systems. We were able to study emulsions with attractive droplets at lower volume fractions with a homogeneous flow profile across the gap (we were also able to create stratified samples but those results are not presented here).

Datta *et al.* studied the detailed yielding behaviour of surfactant-stabilized emulsions with both attractive and repulsive droplets.[10] They found, above random close packing, that the G' values (normalized by the Laplace pressure) are comparable for both types of emulsion; however, the G'' values for emulsions comprised of repulsive droplets are an order of magnitude smaller. In this work the peaks in G'', associated with distinct structural relaxation processes, approaching and during yielding are interrogated. Repulsive emulsions, above random close packing, are found to yield at a strain of $\approx$10% where G'' has a single significant peak. By contrast, attractive emulsions begin to yield at a much lower strain, $\approx$1% and two peaks in G'' are seen. The first peak is at a strain of $\approx$1% while the second is at $\approx$10% as G' and G'' cross. The additional, low strain, peak for attractive emulsions is associated with the breaking of interdroplet bonds, a process that does not need to occur for repulsive droplets.

For our Pickering emulsion samples the G'' signatures, Fig. 2a and 3a, have some similarities and some strong differences with surfactant-stabilized emulsions. The differences are, in part, due to the different droplet sizes studied: Datta *et al.* studied sub-micron droplets[10] while ours are on the scale of tens of microns. Hence their emulsions are Brownian systems while ours are granular. We expect that (elastic) emulsions of similar size, stabilized by molecules, will behave in a similar manner to our emulsions for volume fractions below $\approx$0.85. For higher densities, where our emulsions become unstable, other emulsions might behave differently because the stabilizing molecules may be able to reorganize within the time scale of the deformation. We also observe a low strain ($\approx$1%) peak in G'' for our attractive emulsion droplets which is not seen for our repulsive emulsion. Such peaks, associated with bond breaking, have not only been observed in attractive surfactant-stabilized emulsions[10] but also colloid polymer systems.[20,41,42] By contrast, we do not observe the peak during yielding which dominates the G'' curves for surfactant-stabilized droplets. Miyazaki *et al.*[36] have associated this peak in G'' during yielding with a strong decrease in the α or structural relaxation time as a result of the strain. This means that large collective rearrangements can happen much faster. Because of the granular nature of our system and thus the extremely slow structural relaxation it is not surprising that our system cannot dissipate additional energy (and thus increase G'') through this α relaxation mechanism on the time scale of the oscillation. The most significant G'' peak occurs for us at high strains ($\approx$100%) for both repulsive and attractive Pickering droplets; this is accompanied by a peak in G'. This is a shear thickening signature which is also observed in the moduli of hard sphere dispersions[39] but not for small surfactant-stabilized droplets.[10]

The moduli peaks associated with shear thickening have also been observed in many other systems containing particles such as: hard spheres,[34,43,44] cornstarch[45] and triblock copolymers.[46] In all cases the peaks are also close to 100% strain just as in our system. Other features of the peaks vary in different systems. For our non-Brownian droplets the peaks are expected to remain at all frequencies; for Brownian hard spheres they are found to disappear for low frequencies: here the particles have enough time to move and unjam between collisions. Additionally, because our droplets are soft, the peak heights are not as large as in the case of hard particles. The peaks are even smaller for our attractive emulsions due to the much lower volume fraction of droplets employed. Compared to the results for Brownian hard spheres studied by Petekidis *et al.*[34] we do not observe the loss in correlation caused by Brownian motion in their non-glassy samples. The DWS correlations in their glassy samples show behaviour very similar to our repulsive system, however, the crossing point of their moduli lies very close to the point where their system shear thickens hence they do not distinguish between the effects of the two different processes.

Conclusion

We have demonstrated three different yielding mechanisms in concentrated Pickering emulsions under shear; the mechanism observed depends on volume fraction of droplets and interdroplet interactions. (1) For repulsive emulsions at high volume

fractions yielding occurs when the droplets escape from their cages and start to move irreversibly. In this repulsive glassy system there is no space for (smaller) droplets to escape from their cages while the others remain in place. (2) On the other hand, in a gel-like attractive emulsion, the smaller droplets break their bonds and start to move irreversibly at strains well below the yield strain, resulting in an increase in dissipation and thus an increase in G''. The larger droplets are more strongly bound and as long as they form a percolating network the system remains solid; the system yields when these strong bonds are finally broken. (3) A highly compressed (bi-liquid foam) emulsion on the other hand does not yield by fluidizing instead it yields when the stabilization of the interface fails and the droplets coalesce.

Furthermore, both the fluidized attractive and the repulsive Pickering emulsions show a peak in both G' and G'' at a strain of approximately 100% which is most likely caused by jamming and the resulting shear thickening. This effect is more pronounced for the higher volume fraction Pickering emulsion (repulsive droplets) for which our image analysis reveals the formation of droplet clusters.

A broader comparison reveals that, of the three common signatures in the shear flow of soft particle systems with increasing strain, our granular-scale Pickering emulsions display, at most, two. In order of increasing strain the first signature is a weak strain overshoot (modulus peak) corresponding to the breaking of bonds (typically at small strain 0.1% to 10%), the second is a weak strain overshoot corresponding to an increase in the speed of collective rearrangements (typically before or near the yield point around 1% to 100%) and the third is a strong strain overshoot corresponding to shear thickening resulting from jamming and the formation of system spanning clusters (typically near 100% to 200%). We do not observe the second signature most likely because our droplets are too big and too slow to respond. It would be worthwhile to test this assumption for a Pickering emulsion with smaller droplets and to study the structural rearrangements, in real space, close to the peak in G''.

Acknowledgements

We thank A. Schofield for preparing the particles and R. Besseling for help with rheo-imaging. We gratefully acknowledge J. Thijssen, P. Wilde and W. Poon for useful discussions and comments. Funding was provided by the BBSRC (BB/J500094/1) through the DRINC scheme and by a Royal Society Industry Fellowship.

References

1 F. Leal-Calderon, V. Schmitt and J. Bibette, *Emulsion Science, Basic Principles*, Springer, New York, 2007.
2 S. U. Pickering, Cxcvi. emulsions, *J. Chem. Soc., Trans.*, 1907, **91**, 2001.
3 R. Aveyard, B. P. Binks and J. H. Clint, Emulsions stabilised solely by colloidal particles, *Adv. Colloid Interface Sci.*, 2003, **100**, 503.
4 F. Leal-Calderon and V. Schmitt, Solid-stabilized emulsions, *Curr. Opin. Colloid Interface Sci.*, 2008, **13**, 217.
5 W. Ramsden, *Separation of solids in the surface-layers of solutions and 'suspensions' (observations on surface-membranes, bubbles, emulsions, and mechanical coagulation) – preliminary account*, Proc. Royal Soc., London, vol. 72, 1903, p. 156.
6 T. G. Mason, J. Bibette, D. A. Weitz, *et al.*, Yielding and flow of monodisperse emulsions, *J. Colloid Interface Sci.*, 1996, **179**, 439.
7 T. G. Mason, M.-D. Lacasse, G. S. Grest, D. Levine, J. Bibette and D. A. Weitz, Osmotic pressure and viscoelastic shear moduli of concentrated emulsions, *Phys. Rev. E: Stat. Phys., Plasmas, Fluids, Relat. Interdiscip. Top.*, 1997, **56**, 3150.
8 P. Hébraud, F. Lequeux, J. P. Munch and D. J. Pine, Yielding and rearrangements in disordered emulsions, *Phys. Rev. Lett.*, 1997, **78**, 4657.
9 L. Bécu, S. Manneville and A. Colin, Yielding and flow in adhesive and nonadhesive concentrated emulsions, *Phys. Rev. Lett.*, 2006, **96**, 138302.
10 S. S. Datta, D. D. Gerrard, T. S. Rhodes, T. G. Mason and D. A. Weitz, Rheology of attractive emulsions, *Phys. Rev. E: Stat., Nonlinear, Soft Matter Phys.*, 2011, **84**, 041404.
11 S. Arditty, V. Schmitt, F. Lequeux and F. Leal-Calderon, Interfacial properties in solid-stabilized emulsions, *Eur. Phys. J. B*, 2005, **44**, 381.
12 B. P. Binks, J. H. Clint and C. P. Whitby, Rheological behavior of water-in-oil emulsions stabilized by hydrophobic bentonite particles, *Langmuir*, 2005, **21**, 5307.
13 B. Wolf, S. Lam, M. Kirkland and W. J. Frith, Shear thickening of an emulsion stabilized with hydrophilic silica, *J. Rheol.*, 2007, **51**, 465.
14 W. J. Frith, R. Pichot, M. Kirkland and B. Wolf, Formation, stability, and rheology of particle stabilized emulsions: influence of multivalent cations, *Ind. Eng. Chem. Res.*, 2008, **47**, 6434.
15 B. Braisch, K. Kohler, H. Schuchmann and B. Wolf, Preparation and flow behaviour of oil-in-water emulsions stabilized by hydrophilic silica particles, *Chem. Eng. Technol.*, 2009, **32**, 1107.
16 M. K. Mulligan and J. P. Rothstein, Deformation and breakup of micro- and nanoparticle stabilized droplets in microfluidic extensional flows, *Langmuir*, 2011, **27**, 9760.
17 L. Maurice, R. A. Maguire, A. B. Schofield, M. E. Cates, P. S. Clegg and J. H. J. Thijssen, Squeezing particle-stabilized emulsions into biliquid foams – equation of state, 2013, in preparation.
18 A. J. Liu and S. R. Nagel, Jamming is not just cool any more, *Nature*, 1998, **396**, 21.
19 V. Trappe, V. Prasad, L. Cipelletti, P. N. Segre and D. A. Weitz, Jamming phase diagram for attractive particles, *Nature*, 2001, **411**, 772.
20 K. N. Pham, G. Petekidis, D. Vlassopoulos, S. U. Egelhaaf, W. C. K. Poon and P. N. Pusey, Yielding behavior of repulsion- and attraction-dominated colloidal glasses, *J. Rheol.*, 2008, **52**, 649.

21 H. A. Barnes, Shear-thickening ("dilatancy") in suspensions of nonaggregating solid particles dispersed in newtonian liquids, *J. Rheol.*, 1989, **33**, 329.
22 R. S. Farr, J. R. Melrose and R. C. Ball, Kinetic theory of jamming in hard-sphere startup flows, *Phys. Rev. E: Stat. Phys., Plasmas, Fluids, Relat. Interdiscip. Top.*, 1997, **55**, 7203.
23 C. B. Holmes, M. E. Cates, M. Fuchs and P. Sollich, Glass transitions and shear thickening suspension rheology, *J. Rheol.*, 2005, **49**, 237.
24 T. Blijdenstein, E. van der Linden, T. van Vliet and G. van Aken, Scaling behavior of delayed demixing, rheology, and microstructure of emulsions flocculated by depletion and bridging, *Langmuir*, 2004, **20**, 11321.
25 N. Koumakis, J. F. Brady and G. Petekidis, Complex oscillatory yielding of model hard-sphere glasses, *Phys. Rev. Lett.*, 2013, **110**, 178301.
26 K. A. White, A. B. Schofield, P. Wormald, J. W. Tavacoli, B. P. Binks and P. S. Clegg, Inversion of particle-stabilized emulsions of partially miscible liquids by mild drying of modified silica particles, *J. Colloid Interface Sci.*, 2011, **359**, 126.
27 L. H. Allen and E. Matijević, Stability of colloidal silica: I. effect of simple electrolytes, *J. Colloid Interface Sci.*, 1969, **31**, 287.
28 B. Binks and S. Lumsdon, Stability of oil-in-water emulsions stabilised by silica particles, *Phys. Chem. Chem. Phys.*, 1999, **1**, 3007.
29 R. Besseling, L. Isa, E. R. Weeks and W. C. K. Poon, Quantitative imaging of colloidal flows, *Adv. Colloid Interface Sci.*, 2009, **146**, 1.
30 K. Hyun, M. Wilhelm, C. O. Klein, K. S. Cho, J. G. Nam, K. H. Ahn, S. J. Lee, R. H. Ewoldt and G. H. McKinley, A review of nonlinear oscillatory shear tests: Analysis and application of large amplitude oscillatory shear (laos), *Prog. Polym. Sci.*, 2011, **36**, 1697.
31 R. H. Ewoldt, A. Hosoi and G. H. McKinley, New measures for characterizing nonlinear viscoelasticity in large amplitude oscillatory shear, *J. Rheol.*, 2008, **52**, 1427.
32 J. Lee Rodgers and W. A. Nicewander, Thirteen ways to look at the correlation coefficient, *Am. Stat.*, 1988, **42**, 59.
33 R. Höhler, S. Cohen-Addad and H. Hoballah, Periodic nonlinear bubble motion in aqueous foam under oscillating shear strain, *Phys. Rev. Lett.*, 1997, **79**, 1154.
34 G. Petekidis, A. Moussaïd and P. N. Pusey, Rearrangements in hard-sphere glasses under oscillatory shear strain, *Phys. Rev. E: Stat., Nonlinear, Soft Matter Phys.*, 2002, **66**, 051402.
35 J. Brader, M. Siebenbürger, M. Ballauff, K. Reinheimer, M. Wilhelm, S. Frey, F. Weysser and M. Fuchs, Nonlinear response of dense colloidal suspensions under oscillatory shear: Mode-coupling theory and fourier transform rheology experiments, *Phys. Rev. E: Stat., Nonlinear, Soft Matter Phys.*, 2010, **82**, 061401.
36 K. Miyazaki, H. M. Wyss, D. A. Weitz and D. R. Reichman, Nonlinear viscoelasticity of metastable complex fluids, *Europhys. Lett.*, 2006, **75**, 915.
37 N. Koumakis, A. Pamvouxoglou, A. Poulos and G. Petekidis, Direct comparison of the rheology of model hard and soft particle glasses, *Soft Matter*, 2012, **8**, 4271.
38 E. M. Herzig, A. Robert, D. D. van t' Zand, L. Cipelletti, P. N. Pusey and P. S. Clegg, Dynamics of a colloid-stabilized cream, *Phys. Rev. E: Stat., Nonlinear, Soft Matter Phys.*, 2009, **79**, 011405.
39 J. Mewis and N. J. Wagner, *Colloidal Suspension Rheology*, CUP, Cambridge, 2012.
40 D. Vella, P. Aussillous and L. Mahadevan, Elasticity of an interfacial particle raft, *Europhys. Lett.*, 2004, **68**, 212.
41 M. Laurati, S. Egelhaaf and G. Petekidis, Nonlinear rheology of colloidal gels with intermediate volume fraction, *J. Rheol.*, 2011, **55**, 673.
42 N. Koumakis and G. Petekidis, Two step yielding in attractive colloids: transition from gels to attractive glasses, *Soft Matter*, 2011, **7**, 2456.
43 G. Petekidis, D. Vlassopoulos and P. N. Pusey, Yielding and flow of colloidal glasses, *Faraday Discuss.*, 2002, **123**, 287.
44 N. Koumakis, A. B. Schofield and G. Petekidis, Effects of shear induced crystallization on the rheology and ageing of hard sphere glasses, *Soft Matter*, 2008, **4**, 2008.
45 A. Fall, F. Bertrand, G. Ovarlez and D. Bonn, Shear thickening of cornstarch suspensions, *J. Rheol.*, 2012, **56**, 575.
46 K. Hyun, J. G. Nam, M. Wilhellm, K. H. Ahn and S. J. Lee, Large amplitude oscillatory shear behavior of peo-ppo-peo triblock copolymer solutions, *Rheol. Acta*, 2006, **45**, 239.